

# Maximum-energy records in glassy energy landscapes

Ivailo Hartarsky<sup>\*1</sup>, Marco Baity-Jesi<sup>2</sup>, Riccardo Ravasio<sup>3</sup>, Alain Billoire<sup>4</sup>, and Giulio Biroli<sup>5</sup>

<sup>1</sup>Département Mathématiques et Applications, École Normale Supérieure, CNRS, PSL Research University, 75005 Paris, France

<sup>2</sup>Chemistry Department, Columbia University, 3000 Broadway, 10027 New York (NY), USA

<sup>3</sup>Institute of Physics, École Polytechnique Fédérale de Lausanne, CH-1015 Lausanne, Switzerland

<sup>4</sup>Institut de Physique Théorique, Université Paris Saclay, CNRS, CEA, F-91191, Gif-sur-Yvette, France

<sup>5</sup>Laboratoire de Physique Statistique, École Normale Supérieure, CNRS, PSL Research University, 75005 Paris, France

April 18, 2019

## Abstract

We study the evolution of the maximum energy  $E_{\max}(t)$  reached between time 0 and time  $t$  in the dynamics of simple models with glassy energy landscapes, in instant quenches from infinite temperature to a target temperature  $T$ . Through a detailed description of the activated dynamics, we are able to describe the evolution of  $E_{\max}(t)$  from short times, through the aging regime, until after equilibrium is reached, thus providing a detailed description of the long-time dynamics. Finally, we compare our findings with numerical simulations of the  $p$ -spin glass and show how the maximum energy record can be used to identify the threshold energy in this model.

**Keywords:** Activated dynamics; energy landscapes; extreme value statistics; slow relaxation, glassy dynamics, aging; spin glasses

## Contents

<b>1</b>	<b>Introduction</b>	<b>2</b>
<b>2</b>	<b>Models</b>	<b>3</b>
2.1	Trap model . . . . .	3
2.2	Random Energy Model . . . . .	3
2.3	The $p$ -spin model . . . . .	4
<b>3</b>	<b>Energy maxima in the Trap Model</b>	<b>4</b>
3.1	Qualitative description of the dynamics in the TM . . . . .	4
3.2	Energy Maxima in the Exponential Trap Model . . . . .	5
3.3	Gaussian Trap Model . . . . .	5
<b>4</b>	<b>Energy maxima in the REM</b>	<b>6</b>
4.1	Basic features of the landscape and the dynamics of the REM . . . . .	6
4.2	Energy maximum evolution . . . . .	6
4.2.1	Initial condition . . . . .	6
4.2.2	Drift towards the first trap . . . . .	6
4.2.3	Stay in the first trap . . . . .	7
4.2.4	Reaching common energies . . . . .	7

---

\*ivailo.hartarsky@ens.fr

4.2.5	First new records . . . . .	8
4.2.6	Long time scales: aging regime . . . . .	8
4.2.7	Very long time scales: equilibrium regime . . . . .	9
4.2.8	Saturation . . . . .	9
4.3	Comprehensive view and remarks . . . . .	9
<b>5</b>	<b>Energy maxima and threshold energy in the <math>p</math>-spin model</b>	<b>10</b>
<b>6</b>	<b>Conclusions</b>	<b>11</b>
<b>A</b>	<b>Typical neighbours' energies</b>	<b>13</b>
A.1	Asymptotic bounds . . . . .	13
A.2	Finite $N$ . . . . .	13
<b>B</b>	<b>Corrections for small systems</b>	<b>14</b>
B.1	The initial condition . . . . .	14
B.2	Corrections . . . . .	14
B.2.1	General corrections . . . . .	14
B.2.2	Delayed maximum . . . . .	16
B.2.3	Original maximum . . . . .	17
B.3	Outlook on the finite- $N$ corrections . . . . .	17
<b>C</b>	<b>Records in a single trajectory</b>	<b>18</b>

# 1 Introduction

Record statistics addresses questions on the arising of extreme events in series of random variables [1, 2]. Knowledge of the time scales required for a random process to break a record can be crucial in many fields, such as environment (e.g. probability of floods [3]), finance (e.g. risk estimation), as well as in random walks, evolutionary biology and many more [4].

The simplest case of tracking the maximum in a series of uncorrelated random variables is well understood, but as soon as some correlation is added to the problem, the results become less trivial, and rigorous results are only known for a limited amount of problems, such as simple random walks [2] and eigenvalue statistics [5].

In this work we describe record breaking in *glassy* dynamical systems. These systems usually have a large amount of energy levels, that follow some probability distribution. The main question we address is how long it typically takes for the potential energy to become greater than a fixed amount. Understanding the time evolution of the maximum reached energy  $E_{\max}(t)$  of such systems can help to assess stability limits of a material exposed to a thermal bath (e.g. over a certain energy the material breaks), as well as being strictly related to the aging time scales of the sample. As a matter of fact, it has been recently suggested to rationalize the dynamical slowing down of low-temperature glasses as a record-breaking process over larger and larger domains [6, 7, 8]. Our mean-field results could then account for this process in regions smaller than the correlation length, where the system is effectively fully-connected.

We focus on three paradigmatic models of mean-field glasses, the Trap Model (TM), the Random Energy Model (REM), and the  $p$ -spin model, with particular emphasis on the REM, and study the evolution of the maximum reached energy,  $E_{\max}(t)$ , after an instant quench from an infinite to a small temperature  $T$ .

The TM consists of a random walk in a fully-connected graph in a random potential, where the transition rate does not depend on the destination energy. Here, we find that  $E_{\max}(t)$  has a simple functional form during its whole evolution.

In the REM, the random walk is on a more sparse graph, and the transition rates depend on the difference between the starting and destination energy. This results in a rich non-trivial behavior of  $E_{\max}(t)$ , in which we are able to identify a large amount of different regimes according to the elapsed time. Following  $E_{\max}(t)$  opens a window on exponentially large time scales which are usually hard to study.

Finally, we make a digression to the  $p$ -spin model, whose landscape is more complex than the REM one due to an explicit correlation among the energy levels, which are no longer independent identically distributed (i.i.d.) random variables. We show numerically that even in this case the maximum reached energy grows logarithmically. We also argue that the maximum energy  $E_{\max}(t/2, t)$ , reached in the time interval  $[t/2, t]$ , can be used to identify the threshold energy  $E_{\text{th}}$  (i.e. the highest energy at which local minima are found) in a finite size system, and show numerically that this estimate converges smoothly to its analytical prediction in the thermodynamic limit.

In section 2 we define the models we study. In section 3 we describe the evolution of the maximum reached energy in the TM, whereas in section 4 it is analyzed in the REM. In section 5 we discuss the  $p$ -spin model and the threshold energy. Finally, we give our conclusions in section 6.

## 2 Models

In this section we describe the three models treated in this paper.

### 2.1 Trap model

In the TM [9, 10, 11],  $M$  states lie on a fully connected graph, and their energies are extracted independently from an exponential distribution

$$\rho_{\text{exp}}(E) = \alpha e^{\alpha E} \Theta(-E), \quad (1)$$

where  $\Theta(\cdot)$  is the Heaviside step function and  $\alpha > 0$  is a parameter that will be set to 1.

The transition rate  $q_{i,j}$  from a state  $i$  to a state  $j$  does not depend on the target state  $j$ :

$$q_{i,j} = \frac{1}{M} e^{\beta E(i)}, \quad (2)$$

where  $\beta = 1/T$  is the inverse temperature and  $E(i)$  is the energy of state  $i$ . This represents a system where, to abandon a state (or *trap*), it is necessary to reach a threshold energy  $E_{\text{th}} = 0$ . Once the threshold is reached, the whole space of states becomes accessible. This model has weak ergodicity breaking at temperatures  $T \leq T_c = \frac{1}{\alpha}$  [10] (also see paragraph 3.1).

Summarizing, in the TM the energies of different states are independent, the space of states is fully connected, and the dynamics depends only on the state issuing the transition and not on the target state, implying that there is a constant threshold energy  $E_{\text{th}} = 0$  separating the configurations.

**Gaussian Trap model** The TM can be generalized to a Gaussian energy distribution

$$\rho_{\text{gauss}}(E) = \frac{1}{\sqrt{2\pi N}} e^{-\frac{E^2}{2N}}, \quad (3)$$

setting  $M = 2^N$ . In this case, also positive energies can be reached, but since  $E_{\text{th}} = 0$  they are quickly abandoned with rate given by equation (2).

### 2.2 Random Energy Model

The REM describes a system of  $N$  binary spins [12, 13]. As a consequence, the total number of states is  $M = 2^N$ , and from each configuration it is possible to reach  $N$  new states by flipping a single spin. The energy change induced by flipping any of the spins is assumed to be so drastic, that the energy levels are independent one from the other, and their energy  $E$  is extracted from the probability distribution  $\rho_{\text{gauss}}$  (see Eq. (3)).

The statics of the REM can be solved exactly. There is a disordered phase for temperature  $T > T_c = \frac{1}{\sqrt{2 \ln(2)}}$ , and a glassy phase for  $T < T_c$  [12, 13].<sup>1</sup> Concerning the dynamics, we will

---

<sup>1</sup> The critical temperature  $T_c$  is different from the one given in refs. [12, 13] because we are defining the model with variance  $\text{var}(E) = N$ , instead of  $\text{var}(E) = N/2$ .

focus on Monte Carlo (MC) Metropolis dynamics. More precisely, we consider that spins flip one at a time and we set the transition rate from state  $i$  to state  $j$  to be

$$q_{i,j} = \frac{1}{N} \min\left(1, e^{\beta(E(i)-E(j))}\right). \quad (4)$$

In a nutshell, the REM can be seen as a TM with (i) a hypercubic space of configurations (instead of fully connected), and (ii) with more physical dynamics to move in it. In the limit of very long times and large system sizes, the dynamics of the REM is qualitatively equivalent to the one of the TM, with a threshold energy  $E_{\text{th}} = -\sqrt{2N \ln(N)}$  [14, 15].

### 2.3 The $p$ -spin model

The  $p$ -spin model represents a system of  $N$  binary spins  $\sigma_i = \pm 1$  [12]. Differently from the TM and the REM, where the energies are i.i.d., the energy depends on the microscopic configuration of the system through the Hamiltonian

$$H = - \sum_{i_1 < \dots < i_p} J_{i_1, \dots, i_p} \sigma_{i_1} \dots \sigma_{i_p}, \quad (5)$$

in which the interactions couple all the possible groups of  $p$  different spins. The bonds  $J_{i_1, \dots, i_p}$ , associated to a  $p$ -plet of spins, usually follow a Gaussian or bimodal distribution. We choose the latter, with  $J_{i_1, \dots, i_p} = \pm \sqrt{p!/N^{p-1}}$  with probability one half. An alternative to define the previous Hamiltonian is as a Gaussian random function defined on the  $N$ -dimensional hypercube (in this case the couplings are Gaussian random variables). Its mean is zero, whereas its covariance in the large  $N$  limit is  $\overline{H(\{\sigma_i\})H(\{\sigma'_i\})} \sim Nq^p$  where  $q = \sum_i \sigma_i \sigma'_i / N$ .

When  $p$  is finite, there is general agreement that all models with finite  $p \geq 3$  fall in the same universality class [16]. If instead  $p$  is diverging, the way limits are taken becomes important. On one hand, if one studies the short-time limit, sending first of all  $N \rightarrow \infty$ , and only later  $p, t \rightarrow \infty$ , the  $p$ -spin reduces to the REM [12] (which corresponds naively to saying that in the large  $N$  limit the covariance tends to  $\delta_{\{\sigma_i\}\{\sigma'_i\}}$ ). On the other hand, when studying the long-time regime of activated dynamics, one needs to study large but finite  $N$  at every time  $t$  (recall that by definition  $p \leq N$ ), so the REM cannot be recovered [17].

We will focus on  $p = 3$ , in the limit of large but finite  $N$ , where activated processes become possible [18]. As for the dynamics, we use the single-spin MC Metropolis dynamics, described in Eq. (4).

## 3 Energy maxima in the Trap Model

### 3.1 Qualitative description of the dynamics in the TM

We consider a typical non-equilibrium protocol: an instant quench from infinite temperature to a target temperature  $T$ . In the TM, the system is always stuck in a trap, where it will remain for a time  $\tau \propto e^{-\beta E}$  (Eq. (2)), before emerging to the threshold to transition to the next trap. We call  $\tau$  the trapping time.

One can easily see that the distribution of trapping times is heavy-tailed with density

$$\psi(\tau) \propto \tau^{-(\alpha T + 1)}, \quad (6)$$

which identifies a critical temperature at  $T_c \equiv \frac{1}{\alpha}$  [10]. When  $T < T_c \equiv \frac{1}{\alpha}$  the average trapping time is infinite and the total waiting time is of the order of the maximal waiting time in a single state [10]. Consequently, the process waits in the deepest trap it has seen for about as much time as the system has spent in the heat bath, implying

$$E(t) \approx E_{\text{min}}(t) \sim -T \ln t. \quad (7)$$

Eventually, the system is able to reach  $E_{\text{th}}$  and fall back into shallower traps, until it finds an even deeper trap than the one before, where it spends a time longer than previously elapsed time. As a

consequence, as time passes, the energy decreases gradually, and the dynamics becomes slower and slower. This dependence on how long the system has been in the bath is called *aging* and results in an increasing time correlation of the system. In finite systems aging goes on until equilibrium is reached.

### 3.2 Energy Maxima in the Exponential Trap Model

For our consideration of the maximum energy,  $E_{\max}(t)$ , reached after a time  $t$  we will restrict ourselves to the low-temperature TM, where aging occurs. In other words, we assume that  $T < T_c$ , so that (7) holds. Then  $E_{\max}(t)$  can be calculated through extremum statistics. The number of traps  $n_t$  that the system will have visited must satisfy

$$n_t \int_{-\infty}^{E_{\min}(t)} \rho_{\text{exp}}(E) dE \sim 1, \quad (8)$$

where  $E_{\min}(t)$  is the minimum reached energy at time  $t$ . Therefore,  $n_t \sim e^{-\alpha E_{\min}(t)} \sim e^{-\alpha E(t)}$ , since in the TM the current energy is almost always the lowest reached energy (i.e.  $E(t) \approx E_{\min}(t)$ ).

The number of visited traps needs to satisfy an analogous relation for the largest reached energy

$$n_t \int_{E_{\max}(t)}^0 \rho_{\text{exp}}(E) dE \sim 1, \quad (9)$$

that yields  $n_t \sim -1/E_{\max}(t)$ .

Equating the two expressions for  $n_t$ , and using (7), one obtains the behaviour

$$E_{\max}(t) \sim \ln \left( 1 - t^{-\frac{T}{T_c}} \right) \sim -t^{-\frac{T}{T_c}}, \quad (10)$$

so in the exponential TM the largest reached energy approaches its extremal value  $E = 0$  as a power law.<sup>2</sup>

Note that with respect to all the models defined below, the exponential TM is special (and a bit pathological) since it has a cut-off in the energy distribution at the most numerous energies, i.e. it does not have any rare high-energy. In consequence its behavior is atypical with respect to all other cases considered below.

### 3.3 Gaussian Trap Model

In the Gaussian TM, since  $\rho(E)$  is symmetric, the maximum and minimum records  $E_{\max}(t)$  and  $E_{\min}(t)$  follow the same law, with opposite signs. This is because, from any configuration  $i$ , all the configurations are reached with equal probability, and what changes is only the amount of time the system remains in them. Therefore, a configuration with  $E < E_{\min}(t)$  is reached with the same probability as a configuration with energy  $E > -E_{\min}(t)$ . Since, by Eq. (7), in the TM  $E(t) \sim E_{\min}(t) \sim -T \ln(t)$ , we can deduce that

$$E_{\max}(t) \sim T \ln(t). \quad (11)$$

Eq. (7) still holds for the Gaussian TM in its aging regime,  $t < \exp(\beta\beta_i N)$ , where  $\beta_i = \min(\beta, \beta_c)$  and  $\beta_c = \sqrt{2 \ln 2}$ . If  $\beta < \beta_c$  (i.e. in the high-temperature phase), a supplementary ‘post-equilibration’ regime develops for  $\exp(\beta^2 N) < t < \exp(N(\beta_c^2 + \beta^2)/2)$ , governed by

$$E_{\max}(t) = \sqrt{2N(\ln t - \beta^2 N/2)}. \quad (12)$$

In both cases, the evolution of the maximum energy eventually ends when  $E_{\max}$  reaches the maximum possible value  $N\sqrt{2 \ln 2}$ . As we shall discuss a similar argument for the REM in Sec.4.2.7 and since there is no difference with the minimal energy, we omit the details here. However, let us note that depending on the temperature there are two different behaviours of  $E_{\max}(t)/N$  as a function of  $\ln t/N$ . For  $\beta > \beta_c$  there is a single regime, linear in  $\log(t)$  (11), while otherwise there are two different ones – a linear law (11) followed by a square-root dependency (12).

<sup>2</sup>The high-temperature case,  $T > T_c$ , can be treated similarly, yielding  $E_{\max}(t) \sim -1/t$ .

## 4 Energy maxima in the REM

We now turn to the Metropolis dynamics on the REM and relate it to the TM. Also in this case, we examine quenches from infinite temperature to a target temperature  $T$ . Throughout this section we systematically discard subleading terms. Higher order corrections for finite systems are discussed in App.B.

### 4.1 Basic features of the landscape and the dynamics of the REM

In the REM, most energy levels are concentrated around zero at a typical distance of order  $\sqrt{N}$ . Differently from the TM, the phase space has a structure, and each state has  $N$  neighbours whose energies, as we show in Sec. A.1, Eq. (32), typically lie in the interval

$$I \equiv \left[ -\sqrt{2N \ln N}, \sqrt{2N \ln N} \right]. \quad (13)$$

The majority of states have at least one lower neighbor, and will be quickly abandoned, since the Metropolis update rule [Eq. (4)] privileges energy descent. As a consequence, the states that hold the dynamics most of the time are those without a lower neighbour, which have energy  $\inf I$  or lower. When  $E \sim -N \ll \inf I$ , those states behave like the traps in the TM. In fact, their energy is much lower than the typical energies, so, to leading order, the trapping time in these low configurations scales as  $\tau \sim e^{-\beta E}$  [Eq. (4)].

### 4.2 Energy maximum evolution

In this section, as we did for the TM, we discuss the evolution of the typical maximum energy  $E_{\max}(t)$  in the REM in the limit of very large system sizes. The final results will be summarised in Table 1.

When dealing with exponentially large time scales, a central assumption of our computation is that, each time a state is abandoned, the system becomes independent from its past. In other words, the neighbours are drawn anew so returns to a recently visited configuration are not taken into account. This hypothesis is supported by an argument in Ref. [14], stating that even though, in actual dynamics, earlier configurations are revisited, this happens with a smaller than exponential rate. As a consequence this should not affect exponential time scales.

#### 4.2.1 Initial condition

Before the quench starts, the temperature is infinite, so  $E_{\max}(0)$  is extracted from  $\rho_{\text{gauss}}(E)$ . Therefore, its intensive value is zero in the limit of large system sizes:  $\frac{E_{\max}(0)}{N} \sim \frac{1}{\sqrt{N}} \xrightarrow{N \rightarrow \infty} 0$ .

#### 4.2.2 Drift towards the first trap

At the beginning of the evolution, the system quickly falls into a first local minimum of the energy. See Fig. 1 (left part) for a schematic description of this and the following regimes.

In fact, with probability  $1 - \frac{1}{N+1}$ , the initial state has at least one lower neighbour. The rate  $q_{i,j}$  [Eq. (4)] privileges energy descent, and on time-scales of order one the energy will typically immediately decrease since climbing up moves will be discarded (their rate is exponentially small in  $\sqrt{N}$ ). The transition toward the lowest neighbor, which is at energy  $\inf I$ , has a rate  $q_{i,j} \sim 1/N$ , hence a local minimum will be reached in a time of order  $t_1 = N$  (a configuration at energy  $\inf I$  is a local minimum with probability of order 1). The number of transitions required to reach such state is of order  $\ln(N)$ .<sup>3</sup>

During this regime, before the first trap is reached,  $E_{\max}$  maintains its initial value of order  $\sqrt{N}$ , because the energy is typically descending.

<sup>3</sup>At each transition, the number of lower neighbors is typically divided by two, so it will take  $\mathcal{O}(\log_2(N))$  steps.

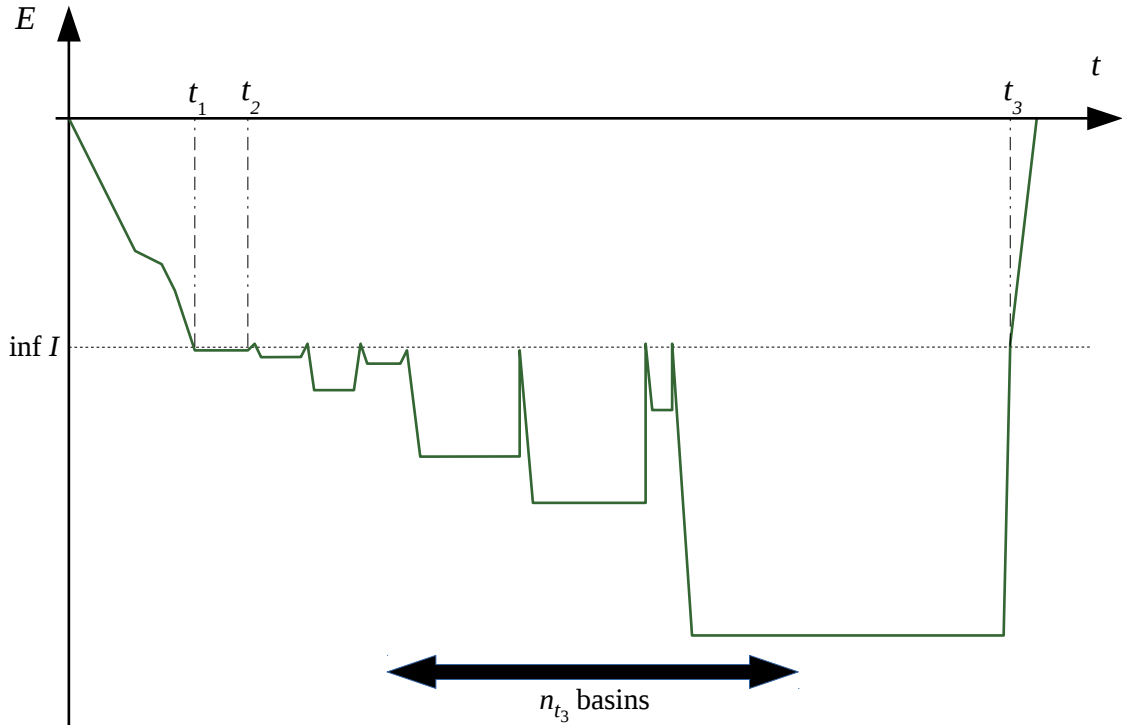


Figure 1: A schematic description of the dynamics of the REM in the initial stages of the dynamics. In a time of order  $t_1 = N$  the system falls in the first local energy minimum. It takes about  $t_2 = \exp(\sqrt{N/\ln N})$  to leave that state. After that, the system will visit a large number of basins,  $n_{t_3}$ , before it can reach energies of order  $\sqrt{N}$ , after a time  $t_3 = e^{\beta E_1}$  [Eq. (17)]. During all this time  $E_{\max}(t) = E(0)$ . The times and energies in the diagram are not in scale.

#### 4.2.3 Stay in the first trap

Once the system reaches the first trap, which has energy  $E \approx \inf I$  (that of a typical lowest neighbour), the energy difference with its neighbours is of order  $\delta = \sqrt{\frac{N}{\ln N}}$  (see App. A.1). Therefore, the system stays stuck in the first trap and does not move at all for a time of the order of  $t_2 = \exp\left(\beta\sqrt{\frac{N}{\ln N}}\right)$ . Consequently,  $E_{\max}(t)$  does not change either.

#### 4.2.4 Reaching common energies

We now estimate the time scale  $t_3$  required, once the first trap is escaped, to climb to energies of order  $\sqrt{N}$ . Such energies need to be reached for a new record  $E_{\max}(t) > E(0) = \mathcal{O}(\sqrt{N})$  to be hit.

After  $t_2$ , the system starts visiting a series of local minima (valleys) of the energy. When these minima are abandoned, they are abandoned through the lowest-energy neighbor of the local minimum, that to leading order is at energy  $\sim \inf I$ . In order to reach energies of order  $\sqrt{N}$ , a large amount of local minima needs to be visited.

The typical trapping time in each of these valleys (which have energy  $E(t)$ ), is

$$\tau_{\text{val}} \sim N e^{\beta(\inf I - E(t))}, \quad (14)$$

and the rate of reaching a configuration of energy  $\mathcal{O}(\sqrt{N})$  by hopping from a local minimum is

$$p_{\text{com}} \sim e^{\beta(E(t) - \mathcal{O}(\sqrt{N}))}. \quad (15)$$

The probability,  $p_3$ , of transitioning in a time  $\tau_{\text{val}}$  to a configuration of energy  $\mathcal{O}(\sqrt{N})$  is given by the product between  $\tau_{\text{val}}$  and  $p_{\text{com}}$ :

$$p_3 \sim \tau_{\text{val}} p_{\text{com}} \sim e^{\beta(\inf I - \mathcal{O}(\sqrt{N}))}. \quad (16)$$

For such a transition to be likely, the number of visited traps  $n_{t_3}$  needs to be of order  $\frac{1}{p_3}$ , since any site usually has numerous neighbours at energy  $\mathcal{O}(\sqrt{N})$ . The lowest of the  $n_{t_3}$  traps gives  $E_{\min}(t)$ : it can be calculated as the minimum among  $Nn_{t_3}$  Gaussians (the factor  $N$  stems from the fact that we are dealing with minima of  $N$  Gaussians, not arbitrary Gaussians) with variance  $N$ , so, through known extremum statistics results (see App. A.1, Eq. (34)), one has

$$-E_{\min}(t_3) \sim \sqrt{2N \ln(Nn_{t_3})} \approx \sqrt{2\beta N \sqrt{2N \ln N}} =: E_1 \quad (17)$$

Through Eq. (7), which is valid also in the REM [14], we obtain  $t_3 = e^{\beta E_1}$ . Until  $t_3$ ,  $E_{\max}(t)$  typically still maintains its initial value.

#### 4.2.5 First new records

After  $t_3$ ,  $E_{\max}(t)$  starts increasing. We address now the regime in which, at every moment, each state has a sizable amount of neighbours with energy higher than the previous record. In other words, at this stage,  $E_{\max}(t) < \sup I$ . The regime ends at a time  $t_4$ , when  $E_{\max}(t_4) \sim \sup I$ .

The way we proceed is analogous to Sec. 4.2.4. When exiting a trap, a neighbour of energy  $E$  is chosen over the lowest one with probability  $p(E) \sim e^{\beta(\inf I - E)}$ . This implies that in order to hit a new record the number of visited traps should be  $n_t \sim \frac{1}{p(E_{\max}(t))}$ . Again, by using extremum statistics (App. A.1, Eq. (34)), one can obtain an expression for the minimum energy,

$$-E_{\min}(t) \approx \sqrt{2\beta N (E_{\max}(t) - \inf I)}. \quad (18)$$

Plugging Eqs. (7) and (13) and (17) into Eq. (18), we obtain

$$E_{\max}(t) = \left( \left( \frac{\ln t}{\beta E_1} \right)^2 - 1 \right) \sqrt{2N \ln N} \quad (19)$$

and solving that for  $E_{\max}(t_4) = \sup I$ , we find  $t_4 = e^{\beta \sqrt{2} E_1}$ .

This stage is followed by a transitory regime after which we can assume  $\sup I \ll E_{\max}(t)$ . We do not treat this transitory regime, because it is analogous to Secs. 4.2.4, 4.2.5 and 4.2.6, and because it concerns subexponential time scales. The interested reader can handle it in the way we just showed, by taking into account that only few traps have a neighbour  $E_{\max}(t) > \sup I$ , with a procedure similar to Sec. 4.2.6.

#### 4.2.6 Long time scales: aging regime

The approach of Secs. 4.2.4 and 4.2.5 can be extended to the whole aging regime, during which a sizeable fraction of time is spent in the deepest trap. In this section we analyze the energy records once  $E_{\max}(t) \gg \sup I$ .

As shown in App. A.1 (see [19]), Eq. (33), basic record statistics imply that the number of traps visited until time  $t$  must satisfy

$$n_t \sim e^{\frac{E_{\min}(t)^2}{2N}}. \quad (20)$$

We can relate  $n_t$  also to  $E_{\max}(t)$ . High-energy configurations are harder to reach, because not only they need to be found, but the transition is also rarely accepted, so  $n_t \sim p\{\text{finding } E_{\max}(t)\}^{-1} \times p\{\text{accepting the transition to } E_{\max}(t)\}^{-1} \equiv p_{\text{find}}^{-1} p_{\text{accept}}^{-1}$ . The rate  $p_{\text{find}}$  is analogous to Eq. (20), since maximal and minimal energies are found (not visited) with the same probability. As for  $p_{\text{accept}}$ , the dynamics has a probability  $p(E_{\max}(t)) \sim e^{\beta(\inf I - E_{\max}(t))} \approx e^{-\beta E_{\max}(t)}$  to accept a transition to a neighbour of energy  $E_{\max}(t)$ . Therefore,

$$n_t \sim e^{\frac{E_{\max}(t)^2}{2N}} e^{\beta E_{\max}(t)}. \quad (21)$$



Putting together (7), (20) and (21) we get

$$E_{\max}(t) = -\beta N + \sqrt{N^2\beta^2 + \beta^{-2}(\ln t)^2}. \quad (22)$$

In order to determine the end of aging  $t_5$ , we consider the mean energy, which is equal to  $E_{\min}(t)$  as long as aging lasts. Then aging ends with  $E_{\min}(t_5) = -\frac{\ln t_5}{\beta}$  equal to the equilibrium mean energy, itself given either by the global minimum of the energy or by  $\langle E \rangle = \frac{\int E e^{-\beta E} \rho_{\text{gauss}}(E) dE}{\int e^{-\beta E} \rho_{\text{gauss}}(E) dE} = -\beta N$ . Hence, by App. A.1, (31)

$$t_5 = e^{\beta\beta_i N}, \quad (23)$$

where we introduced  $\beta_i \equiv \min(\beta, \beta_c)$ .

**Logarithmic growth.** Notice that this regime is the most relevant in our description, since it describes the aging occurring at exponential time scales, that in the thermodynamic limit are the relevant ones.  $E_{\max}(t)$  grows as  $\ln(t)$  (and so does  $-E_{\min}(t)$ ) until the system has eventually equilibrated. Yet, since, the growth of  $E_{\max}(t)$  is slower, it will keep growing even after  $E_{\min}(t)$  saturated.

#### 4.2.7 Very long time scales: equilibrium regime

$E_{\max}(t)$  continues to evolve even though the system has already reached macroscopic equilibrium. In this regime Eq. (21) still holds, whereas Eq. (7) fails.

The calculation that led to Eq. (23) also gives that the mean time spent per state  $\frac{t}{n_t}$  stations at the end of aging (the system reaches macroscopic equilibrium) at the value  $\frac{t_5}{n_{t_5}}$ . In other words,  $\frac{t}{n_t} = \frac{t_5}{n_{t_5}}, \forall t > t_5$ .

Using (20) and (23), we have  $t = n_t \frac{t_5}{n_{t_5}} = n_t e^{\beta\beta_i N} e^{-N\frac{\beta_i^2}{2}}$ . Thus, by replacing  $n_t$  with its explicit expression in Eq. (21), one obtains

$$E_{\max}(t) = -\beta N + \sqrt{(\beta - \beta_i)^2 N^2 + 2N \ln t}. \quad (24)$$

Eq. (24) is valid until the global maximum  $E_{\max}(\infty) = \beta_c N$  (see App. A.1, Eq. (31)) is reached. This means that remains valid for

$$\ln t \leq (2\beta - \beta_i + \beta_c)(\beta_c + \beta_i) \frac{N}{2} = \begin{cases} N \frac{(\beta + \beta_c)^2}{2} & \text{if } \beta < \beta_c \\ 2N\beta_c\beta & \text{if } \beta > \beta_c. \end{cases} \quad (25)$$

Inequality (25) defines the typical time  $t_6$  required to reach the global maximum

$$t_6 = e^{(2\beta - \beta_i + \beta_c)(\beta_c + \beta_i) \frac{N}{2}}. \quad (26)$$

#### 4.2.8 Saturation

Naturally, after  $t_6$ , that is after the global maximum has been attained, the maximum energy cannot change anymore, so

$$E_{\max}(t) = \beta_c N. \quad (27)$$

### 4.3 Comprehensive view and remarks

In our discussion, we treated the typical maximum of the energy  $E_{\max}(t)$ . We expect that when taking the thermodynamic limit there will be a concentration of the measure around a central value, so the same results should hold when replacing typical  $E_{\max}(t)$  by the expectation  $\mathbb{E}[E_{\max}(t)]$ . In App. B, we describe the subleading corrections that need to be taken into account in order to study finite systems, and tackle a few of them. The different regimes of  $E(t)$  and  $E_{\max}(t)$  (at leading order) are summarized in Tab. 1.

Relevant time scales for the glassy activated dynamics stem naturally from our analysis. The longest time scale is exponentially large in the system size. Thus, we can define a rescaled time

Regime	$\ln(t_{\text{end}})$	$E(t)$	$E_{\text{max}}(t)/N$
Initial	0	$\sim \sqrt{N}$	$E(0)/N$
Drift	$\ln N$	decreasing	$E(0)/N$
First trap	$\beta \sqrt{\frac{N}{\ln N}}$	$\inf I$	$E(0)/N$
Common	$\beta E_1$	$-T \ln t$	$E(0)/N$
First records	$\beta \sqrt{2} E_1$	$-T \ln t$	$\left( \left( \frac{\ln t}{\beta E_1} \right)^2 - 1 \right) \sqrt{\frac{2 \ln N}{N}}$
Aging	$\beta \beta_i N$	$-T \ln t$	$-\beta + \sqrt{\beta^2 + \left( \frac{\ln t}{\beta N} \right)^2}$
Equilibrium	$(2\beta - \beta_i + \beta_c)(\beta_c + \beta_i) \frac{N}{2}$	$-\beta_i N$	$-\beta + \sqrt{(\beta - \beta_i)^2 + 2 \frac{\ln t}{N}}$
Saturation	$\infty$	$-\beta_i N$	$\beta_c$

Table 1: Summary of the regimes of the dynamics evolution in the REM. For each regime (first column) we depict the logarithm of the time until when the regime is valid,  $\ln(t_{\text{end}})$ , the typical energy one finds at time  $t$ ,  $E(t)$ , and the typical record of the maximum energy,  $E_{\text{max}}(t)$ . The energy  $E_1 = \sqrt{2\beta N \sqrt{2N \ln N}}$  is defined in Eq. (17),  $\beta_c = 1/T_c$  is the inverse critical temperature, and  $\beta_i = \min(\beta_c, \beta)$ .

$\theta = \ln t/N$ , which is useful to express Eqs. (22), (24) and (27) in a meaningful way. The intensive maximum energy for these time scales is plotted in Fig. 2–left, with a comparison with numerics in small systems. In the thermodynamic limit, the piecewise concatenation of these regimes is continuous.<sup>4</sup>

In units of  $\theta$ , all the previous time regimes collapse to zero in the thermodynamic limit. For the regime at which the first records are observed, the relevant rescaled time is  $\theta' = \ln t/(\beta E_1(N))$ , whereas the energy should be rescaled by a factor  $1/\sqrt{2N \ln N}$  [see Eq. (19)]. The resulting rescaled curve is plotted in the inset of Fig. 2–left.

In Fig. 2–right, we show that  $E_{\text{max}}(t)$  keeps growing even after the system has thermalized, and that the equilibration time,  $t_5$ , extracted from  $E_{\text{max}}(t)$  (in the thermodynamic limit) corresponds roughly to the time at which  $E(t)$  reaches its equilibrium value (in a system of size  $N = 12$ ).

## 5 Energy maxima and threshold energy in the $p$ -spin model

A natural question is how the behavior of  $E_{\text{max}}(t)$  extends to more complex glassy systems, and what it can teach about them. We consider the  $p$ -spin model, since in the limit  $p \rightarrow \infty$  the thermodynamics (though not the long-time activated dynamics [17]) is the same as the one of the REM.

In the  $p$ -spin model, there is a threshold energy  $E_{\text{th}}$  over which there are no energy minima [20], as it also happens in the TM and the REM. Yet, differently from the TM and the REM, where  $\lim_{N \rightarrow \infty} (E_{\text{th}}/N) = 0$ , in the  $p$ -spin model  $E_{\text{th}}$  is intensively negative (i.e.  $\lim_{N \rightarrow \infty} (E_{\text{th}}/N) < 0$ ).

Let us now take into account the maximum energy  $E_{\text{max}}(t/2, t)$  reached in the time interval  $[t/2, t]$ . Taking the maximum in a dilating time interval is useful to identify the separation of time scales that arises in the dynamics of glassy systems. In the thermodynamic limit, the dynamics of the  $p$ -spin model on time scales not diverging with  $N$  is known [21]: the intensive energy decreases monotonically towards the threshold energy. Moreover, in this regime, the energy as a function of time has fluctuations of order  $N^{-1/2}$ . In consequence,  $E_{\text{max}}(t/2, t)$  is equal to the intensive energy at time  $t/2$  and approaches  $E_{\text{th}}$  for  $t \gg 1$  but not diverging with  $N$ . On times diverging with  $N$  the dynamics becomes activated (on time-scales exponentially large in  $N$ ), the intensive energy goes below  $E_{\text{th}}$ , and the energy starts to have rare high-excursions that make increase the value of  $E_{\text{max}}(t/2, t)$  (see also Fig. 5 in App. C). Hence, one can expect that  $E_{\text{max}}(t/2, t)$  grows close to logarithmically, as in record-breaking dynamics for i.i.d. random variables (and as it happens for

<sup>4</sup>For  $\beta < \beta_c$  its derivative is also continuous at  $\theta = \beta \beta_i$ , corresponding to  $t_5$ .

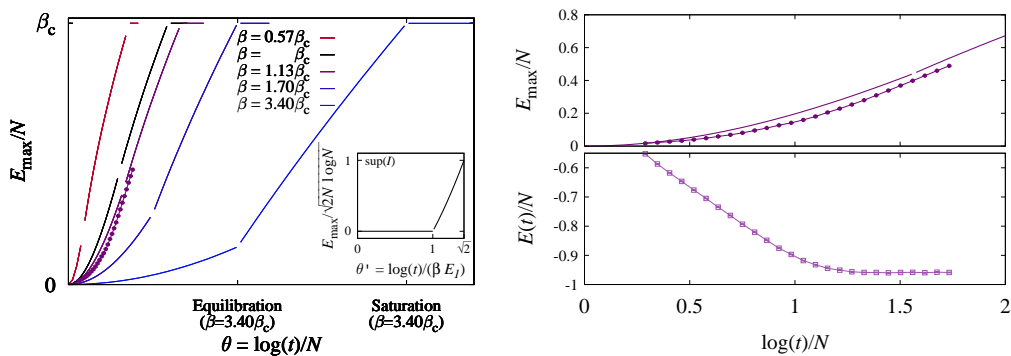


Figure 2: **Left:** Intensive maximum energy,  $E_{\max}$ , as a function of the rescaled time  $\theta = \ln t/N$ , for several values of the inverse temperature  $\beta$ . The  $y$  axis is linear, in units of  $\beta_c$ . The curves are split in three, in order to stress the presence of three subsequent regimes: Aging (Sec. 4.2.6), Equilibrium (Sec. 4.2.7) and Saturation (Sec. 4.2.8). The ticks on the  $x$  axis show the beginning of these regimes for the highest  $\beta$ , corresponding to  $T = 0.25$ . We also show data from simulations at  $\beta = 1.13\beta_c$ , for systems of size  $N = 12$ , which agrees well with our  $N = \infty$  predictions. Finite-size corrections are discussed in App. B. In the **inset** we show  $E_{\max}$  for shorter time scales  $\theta'$  (see main text). **Right:** The **top** figure depicts the same curves shown on the left panel, for  $\beta = 1.13\beta_c$ . The solid line is the result of our calculation (in the thermodynamic limit), and the points are from runs with  $N = 12$  (error bars are smaller than the points). The separation between the continuous lines emphasizes the end of the aging regime according to our calculation [Eq. (23)]. The **bottom** figure shows the energy as a function of time. Numerical data here and in Fig. 3 are averaged over disorder realizations.

$E_{\max}(t)$  in the REM during the aging regime, see table 1).

The minimum value reached by  $E_{\max}(t/2, t)$  can be used to define the value of  $E_{\text{th}}$  in numerical simulations. In Fig. 3 we show  $E_{\max}(t/2, t)$  both in the REM and in the  $p$ -spin model (with  $p = 3$ ), for different system sizes. As expected, in both cases the curve reaches a minimum which we identify as  $E_{\text{th}}$ . Note that, in the REM,  $\frac{E_{\text{th}}}{N}$  grows as  $N$  increases whereas in the 3-spin model it decreases, in agreement with the fact that the intensive threshold energy is zero in the former model and negative in the latter. In the inset of Fig. 3, we show that, in the  $p$ -spin model,<sup>5</sup> the finite-size threshold energy obtained through this procedure is controlled by the  $N^{-1/2}$  fluctuations, and converges to its analytical value in the thermodynamic limit [22]. From the figure one can also see that, as argued in the previous paragraph, the relevant time scales for the growth of  $E_{\max}(t/2, t)$  are exponential.

## 6 Conclusions

By counting the number of visited traps, and remarking that in TM-like models almost all the time is spent in the deepest trap, we were able to calculate the evolution of the maximum reached energy after a time  $t$ . This provided a window on the long-time behavior of glassy systems, which is a notoriously hard and poorly understood regime of the dynamics. Moreover, a distinction between short and long-time regimes arises spontaneously from the behavior of  $E_{\max}(t)$ .

The more complicated phenomenology of the REM with respect to the TM is the result of the more realistic Metropolis dynamics and the sparsity of the underlying graph connecting configurations.

In models where it is not known whether it is necessary to reach a well-defined threshold energy to abandon a basin, this kind of analysis is harder analytically, but in principle can be done numerically, by using the threshold energy defined by the minimum value of  $E_{\max}(t/2, t)$ , which gives a reasonable estimate in REM and  $p$ -spin model.

<sup>5</sup>This same scaling is not as clean in the REM, probably because the system sizes are too small. In App. B we argue that the asymptotic limit is reached for  $N \sim 10^3$ .

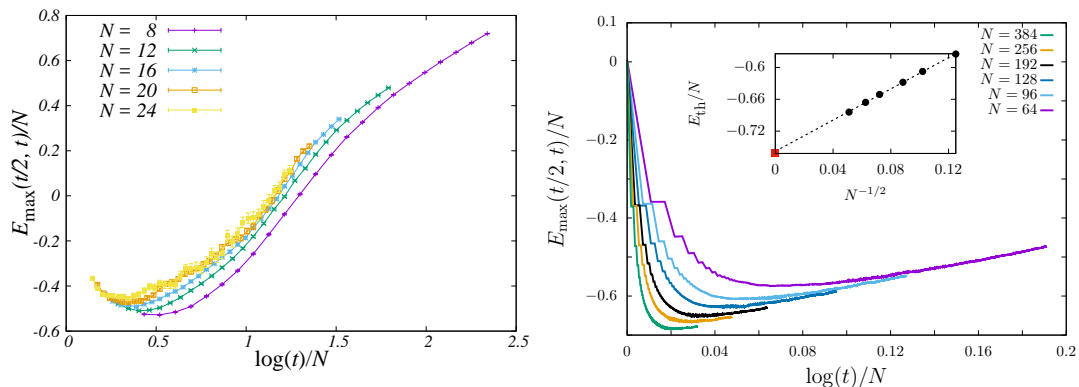


Figure 3: Intensive maximum energy  $E_{\max}(t/2, t)/N$  reached in the time interval  $[t/2, t]$ , for different system sizes  $N$ . On the **left**, we show data for the REM at  $T = 0.75$ . Decreasing the temperature (not shown), the bottom of curve becomes progressively flatter, but the lowest point stays approximately at the same height. On the **right**, we show data for the 3-spin model at  $T = 0.54$ . In both cases the curves seem to converge to a master curve proportional to  $\ln(t)$ . **Inset:** Scaling behaviour of the size-dependent threshold energy  $E_{\text{th}}(N)$  (defined as the minimum of  $E_{\max}(t)$ ) in the 3-spin model. The prediction from Ref. [22], valid for infinitely large systems,  $E_{\text{th}} = -0.762$ , is also shown (red square). The dotted line represents the fit  $E_{\text{th}}(N) = aN^{-1/2} + b$ . The coefficients of the fit are  $a = 1.47(1)$  and  $b = -0.758(1)$  [22].

## Acknowledgements

We thank Valerio Astuti, Chiara Cammarota, Claude Godrèche and Satya Majumdar for interesting discussions. This work was funded by the Simons Foundation for the collaboration “Cracking the Glass Problem” (No. 454935 to G. Biroli and No. 454951 to D.R. Reichman). M.B.-J. was partially supported through Grant No. FIS2015-65078-C2-1-P, jointly funded by MINECO (Spain) and FEDER (European Union).”

## A Typical neighbours' energies

In this section we recall some useful results from extremum statistics that we use thorough in our paper. For a more detailed discussion we refer, for example, to Ref. [1].

### A.1 Asymptotic bounds

We want to find the typical value of the maximum  $M_n$ , out of  $n$  i.i.d. random variables extracted from distribution  $\rho_{\text{gauss}}(E)$  [Eq. (3)].

Let  $X$  be a random variable from the distribution  $\rho_{\text{gauss}}$ . Its cumulative distribution  $F(x)$  is the probability that  $X$  is smaller than  $x$ ,  $F(x) = \mathbb{P}(X \leq x)$ . We consider i.i.d. random variables, so the probability that the maximum of  $n$  tries is smaller than some constant  $a$  is  $\mathbb{P}(M_n \leq a) = (F(a))^n$ .

We can find a location-scale transformation to show that  $M_n$  asymptotically follows the Gumbel distribution  $\mathcal{L}_{\text{GUM}}((-\infty, x]) = e^{-e^{-x}}$ .<sup>6</sup> Set

$$a_n = \sqrt{\frac{N}{2 \ln n}}, \quad b_n = \sqrt{2N \ln n} \left( 1 - \frac{\ln \ln n + \ln(4\pi)}{4 \ln n} \right). \quad (28)$$

Then integrating by parts we get

$$\begin{aligned} 1 - F(b_n + xa_n) &= \frac{1}{\sqrt{2\pi N}} \int_{b_n + xa_n}^{\infty} e^{-\frac{y^2}{2N}} dy \stackrel{n \rightarrow \infty}{\sim} \sqrt{\frac{N}{2\pi}} e^{-\frac{(b_n + xa_n)^2}{2N}} \frac{1}{b_n + xa_n} \\ &\sim \frac{1}{\sqrt{4\pi \ln n}} \exp\left(-x - \frac{b_n^2}{2N}\right) \sim \frac{e^{-x}}{n}. \end{aligned} \quad (29)$$

By isolating  $F(b_n + xa_n)$  and recalling that  $\mathbb{P}(M_n \leq a) = (F(a))^n$ , one gets that

$$\mathbb{P}\left(\frac{M_n - b_n}{a_n} \leq x\right) \stackrel{n \rightarrow \infty}{\rightarrow} \mathcal{L}_{\text{GUM}}. \quad (30)$$

The particular cases we are interested in this paper are  $n = 2^N$  and  $n = N$ . By replacing the former in  $b_n$ , we get that, when  $n = 2^N$ , the global maximum of the energy is

$$E_{\text{max}}(\infty) = -E_{\text{min}}(\infty) = M_{2^N} = \beta_c N + \mathcal{O}(\ln N). \quad (31)$$

The second case,  $n = N$ , reproduces the maximum energy among the neighbors of a configuration,

$$-\inf I = \sup I = M_N = \sqrt{2N \ln N} \left( 1 + \mathcal{O}\left(\frac{\ln \ln N}{\ln N}\right) \right). \quad (32)$$

Moreover, to the leading order Eq. (30) gives

$$n \approx e^{\frac{M_n^2}{2N}} \quad (33)$$

or equivalently

$$M_n \approx \sqrt{2N \ln n}. \quad (34)$$

It is worth noting that, according to Eq. (30), the energy difference between a local minimum and its lowest neighbour is of order  $a_N$ . Moreover, due to the concentration of  $M_n$  on  $b_n$ , for large systems one can treat both the global maximum of the energies and  $I$  in a deterministic way.

### A.2 Finite $N$

When dealing with small systems (see App. B) we need to go beyond the asymptotic bounds. To get the exact expression for  $\sup(I) = M_N$  we can use again the fact that  $\mathbb{P}(M_n \leq x) = (F(x))^n$ , from where we can extract the distribution of  $M_n$ , and calculate its average, which results in

$$\sup I = -\inf I = \sqrt{\frac{N}{2\pi}} \int_{-\infty}^{+\infty} Nx(1 - \text{erfc}(x))^{N-1} e^{-\frac{x^2}{2}} dx, \quad (35)$$

<sup>6</sup>Mind that the Gumbel distribution is not centered: its mean is the Euler-Mascheroni constant  $\gamma$ .

where

$$\operatorname{erfc}(x) = \frac{1}{\sqrt{2\pi}} \int_x^\infty e^{-\frac{u^2}{2}} du. \quad (36)$$

For example, for  $N = 20$ , this gives  $\sup I \approx 8.34$ .

## B Corrections for small systems

In this appendix we take into account subleading terms of  $E_{\max}(t)$ , so as to make quantitative predictions also for small system sizes. The general reasoning will remain the same as in Sec. 4, but we will pay particular attention to the fact that  $\inf I \ll N$  and we will no longer use the asymptotic value of  $\inf I$ , in favor of Eq. (35).

### B.1 The initial condition

It is convenient to study not only  $\mathbb{E}[E_{\max}(t)]$  – the expectation over different instances of the REM – but also the expectation given the starting energy  $\mathbb{E}[E_{\max}(t)|E(0)]$ . A particular case that will be useful in the following, is when the dynamics starts at the threshold energy,

$$\mathcal{E}(t) := \mathbb{E}[E_{\max}(t)|E(0) \approx \inf I]. \quad (37)$$

From  $\mathcal{E}(t)$  we can compute  $E_{\max}$  from any starting condition. If  $E(0) < \inf I$  we have

$$\mathbb{E}[E_{\max}(t)|E(0)] = \begin{cases} E(0) & \text{if } t \ll e^{\beta(\inf I - E(0))} \\ \mathcal{E}(t - e^{\beta(\inf I - E(0))}) \approx \mathcal{E}(t) & \text{if } t \gg e^{\beta(\inf I - E(0))}, \end{cases} \quad (38)$$

whereas if  $E(0) > \inf I$  and  $t \gg N$  we get

$$\mathbb{E}[E_{\max}(t)|E(0)] = \max(E(0), \mathcal{E}(t)). \quad (39)$$

$\mathcal{E}(0)$  can be regarded as the energy reached after time scales of order  $t_1 = N$  (Sec. 4). Hence, studying  $\mathcal{E}(t)$  is equivalent to looking at  $\mathbb{E}[E_{\max}(t)]$ , disregarding the initial part of the dynamics (any time before the first trap is abandoned). This time delay is small compared to the other time scales in play.

### B.2 Corrections

#### B.2.1 General corrections

The main finite-size corrections we treat are

- Finite-size corrections to extreme value results.
- Typical depth of traps.
- Alternative paths for reaching high energies.

Further corrections that we did not take into account are stressed in Sec. B.3.

**Finer analysis of traps and their barriers** Consider a local minimum of the energy landscape and denote its energy by  $E$ . Then  $E$  is simply the minimum of  $N + 1$  energies from  $\rho_{\text{gauss}}$ , which is close to  $\inf I$ . However, attention should be paid to the energy of its lowest neighbour, which is not simply  $\inf I$ , since it is conditioned to be at energy higher than  $E$ . The average energy  $\phi(E)$  of the lowest neighbor of a configuration with energy  $E$  should then be rewritten as

$$\phi(E) = \frac{\sqrt{N} \int_{\frac{E}{\sqrt{N}}}^\infty x(1 - \operatorname{erfc}(x))^{N-1} e^{-\frac{x^2}{2}} dx}{\int_{\frac{E}{\sqrt{N}}}^\infty (1 - \operatorname{erfc}(x))^{N-1} e^{-\frac{x^2}{2}} dx}. \quad (40)$$

The function  $\phi(E)$  goes down from an initial value a bit higher than  $\inf I$ , when  $E = \inf I$ , to  $\inf I$ , when  $E$  is a few standard deviations of  $\inf I$  lower than it. In particular, by the end of aging we can safely write  $\phi(\mathcal{E}_{\min}(t)) = \inf I$ , since the system will have reached the lowest-energy configuration.

Using Eq. (40), the exit time of a trap, that corresponds approximately to the mean time required to go to the lowest neighbour, is rewritten as

$$t_{\text{exit}} = N e^{\beta(\phi(E) - E)}. \quad (41)$$

**Aging regime** During the aging stage, since most of the time is spent in the lowest state, the total elapsed time can be expressed as

$$t_{\text{exit}}^{(\text{aging})} \approx N e^{\beta[\phi(\mathcal{E}_{\min}(t)) - \mathcal{E}_{\min}(t)]}. \quad (42)$$

Hence, taking into account the relations in App. A.1, the aging now ends after a time of order

$$t'_5 = N e^{\beta(\inf I + \beta_i N)} \left( \sqrt{2\pi N} \beta_i e^{-\gamma} \right)^{-\frac{\beta}{\beta_i}}, \quad (43)$$

where we also centered the Gumbel distribution, which gives the  $\gamma$  term, and used  $\phi(\mathcal{E}_{\min}(t'_5)) \approx \inf I$ . Retaining just the main order gives

$$t_5^{(0)} = e^{\beta(\inf I + \beta_i N)}. \quad (44)$$

**Time at lowest neighbours** The time spent in *lowest neighbours* of traps is about  $N n_t$ , since due to the Metropolis rate (4) the time spent before leaving them is of order  $N$ . Recall that if one draws  $N n_t$  energies from  $\rho_{\text{gauss}}$ , their minimum is distributed as the minimum of  $n_t$  lowest neighbours (see also Sec. 4.2.4). Then, according to Eqs. (28) and (30) in Sec. A.1, defining  $y \equiv \ln(N n_t)$ , one has

$$\mathcal{E}_{\min}(t) = \sqrt{2N y} \left( 1 - \frac{\ln y + \ln(4\pi) - 2\gamma}{4y} \right).$$

The second term on the right hand side is small, so it can be treated as a perturbation. To the first order, one obtains

$$\ln(N n_t) = \frac{\mathcal{E}_{\min}^2(t)}{2N} \left( 1 + N \frac{\ln \frac{\mathcal{E}_{\min}^2(t)}{2N} + \ln(4\pi) - 2\gamma}{\mathcal{E}_{\min}^2(t)} \right). \quad (45)$$

**Records via other neighbours** As most of the time is spent at the bottom of traps, a new record  $E$  for the maximum energy can be attained either transiting directly from the bottom of the trap,  $E_{\text{trap}}$ , or via one of its neighbours. Let us denote by  $A(E)$  the probability that  $E$  is reached from the trap or its neighbours divided by the probability that it is reached directly from the trap.

The probability of reaching  $E$  directly from the trap is given by the time spent there,

$$N \exp(\beta(\phi(E_{\text{trap}}) - E_{\text{trap}})),$$

times the transition rate  $\exp(\beta(E_{\text{trap}} - E))/N$ . Let us consider the lowest neighbour,  $\phi(E_{\text{trap}})$ , which typically has two neighbours (including the trap) with lower energy. It has exactly half the transition probability to  $E$  as directly from the trap, because the less time spent in it,  $N/2$ , cancels out with the higher transition rate towards  $E$ . The second-lowest energy has typically three lower neighbours, so by the same reasoning it contributes as a third of the direct transition from the trap. Continuing this way we get a total transition rate of  $H_n$  times the one directly from the trap, where  $H_n$  is the harmonic partial sum.

However, this reasoning only concerns the neighbours of the trap with energies lower than  $E$ . In the general case we get

$$A(E) \approx \max \left( \ln \left( N \text{erfc} \left( \frac{-E}{\sqrt{N}} \right) \right), 1 \right), \quad (46)$$

where we approximate  $H_n$  by  $\ln n$  and recall the fact that transiting directly from the trap is always possible to avoid errors for  $E$  close to  $\inf I$ .

## B.2.2 Delayed maximum

**Long-time aging regime** Note that most of the lowest neighbours of traps visited are at energy  $\phi(\inf I)$ . Then, due to the previous observations  $\mathcal{E}(t)$  should satisfy, analogously to Sec. 4.2.6,

$$\begin{aligned}
1 &\simeq Nn_t \int_{\mathcal{E}(t)}^{\infty} A(E)q_{\phi(\inf I),E}N\rho_{\text{gauss}}(E)dE \\
&\approx e^{-\gamma} \sqrt{\frac{2\pi\mathcal{E}_{\min}^2(t)}{N}} e^{\frac{\mathcal{E}_{\min}^2(t)}{2N}} A(\mathcal{E}(t)) \int_{\mathcal{E}(t)}^{\infty} \frac{1}{N} e^{\beta(\phi(\inf I)-E)} N\rho_{\text{gauss}}(E)dE \\
&\approx e^{-\gamma} A(\mathcal{E}(t)) \frac{\sqrt{N}|\mathcal{E}_{\min}(t)|}{(\mathcal{E}(t) + \beta N)\sqrt{2\pi}} \sqrt{\frac{2\pi}{N}} e^{\frac{\mathcal{E}_{\min}^2(t)}{2N}} e^{\beta(\phi(\inf I)-\mathcal{E}(t))} e^{-\frac{\mathcal{E}^2(t)}{2N}} \\
&\approx e^{-\gamma} B(\mathcal{E}(t)) \frac{|\mathcal{E}_{\min}(t)|}{\beta N} e^{\frac{\mathcal{E}_{\min}^2(t)}{2N}} e^{\beta(\phi(\inf I)-\mathcal{E}(t))} e^{-\frac{\mathcal{E}^2(t)}{2N}},
\end{aligned} \tag{47}$$

where  $q_{i,j}$  is the Metropolis rate from state  $i$  to state  $j$ , and in the last step we set

$$B(E) := \frac{A(E)}{1 + \frac{E}{\beta N}}. \tag{48}$$

Notice that the subexponential terms are only very small perturbations, so one can still solve the transcendental equation. Then, combining (42) and (47) yields at the main order

$$\mathcal{E}^{(0)}(t) \approx -\beta N + \sqrt{(\beta N + \inf I)^2 - 2\frac{1}{\beta} \inf I \ln t + \left(\frac{1}{\beta} \ln t\right)^2}. \tag{49}$$

At this point, one can use Eqs. (48) and (49) in the bottom line of Eq. (47), to solve it recursively, obtaining

$$\begin{aligned}
\mathcal{E}(t) &\approx -\beta N + \left( \beta^2 N^2 + 2\beta N \phi(\inf I) + (\mathcal{E}_{\min}(t))^2 \right. \\
&\quad \left. + 2N \ln \frac{\mathcal{E}_{\min}(t)}{\beta N} + 2N \ln B(\mathcal{E}^{(0)}(t)) - 2N\gamma \right)^{\frac{1}{2}}.
\end{aligned} \tag{50}$$

where we used that  $\phi(\mathcal{E}_{\min}) = \inf I$ , so this expression can only be valid deep in the aging regime.

**Equilibrium regime** After the end of aging ( $t > t'_5$ , Eq. (43)) we use that the mean time spent per state stations at its value at the end of aging  $\frac{t'_5}{n_{t'_5}}$ . Also, at the end of aging one has

$Nn_{t'_5} \approx e^{\frac{N\beta_1^2}{2}}$ . Hence, following Eq. (43),

$$\begin{aligned}
1 &\simeq t \frac{Nn_{t'_5}}{t'_5} \int_{\mathcal{E}(t)}^{\infty} A(E)q_{\phi(\inf I),E}N\rho_{\text{gauss}}(E)dE \approx \\
&\approx \frac{t}{N} e^{-\beta(\beta_1 N + \inf I)} \left( \sqrt{2\pi N} \beta_1 e^{-\gamma} \right)^{\frac{\beta}{\beta_1}} e^{\frac{N\beta_1^2}{2}} A(\mathcal{E}(t)) \cdot \int_{\mathcal{E}(t)}^{\infty} e^{\beta(\phi(\inf I)-E)} \rho_{\text{gauss}}(E)dE \approx \\
&\approx \frac{\sqrt{N}A(\mathcal{E}(t))}{(\mathcal{E}(t) + \beta N)\sqrt{2\pi}} \left( \sqrt{2\pi N} \beta_1 e^{-\gamma} \right)^{\frac{\beta}{\beta_1}} \frac{t}{N} e^{-\beta\beta_1 N} e^{\frac{N\beta_1^2}{2}} \cdot e^{-\beta\mathcal{E}(t)} e^{-\frac{\mathcal{E}^2(t)}{2N}} e^{\beta(\phi(\inf I)-\inf I)} \approx \\
&\approx C(\mathcal{E}(t)) \left( \sqrt{2\pi N} \beta_1 \right)^{\frac{\beta}{\beta_1}-1} e^{-\frac{\gamma\beta}{\beta_1}} \frac{t}{N} e^{-\beta\beta_1 N} e^{\frac{N\beta_1^2}{2}} e^{-\beta\mathcal{E}(t)} e^{-\frac{\mathcal{E}^2(t)}{2N}} e^{\beta(\phi(\inf I)-\inf I)},
\end{aligned} \tag{51}$$

where in the last step we set

$$C(E) := A(E) \frac{\beta_1}{\beta + \frac{E}{N}}. \tag{52}$$



Like in the previous paragraph, neglecting subexponential factors and solving (51) for  $\mathcal{E}(t)$  gives the main order

$$\frac{\mathcal{E}^{(0)}(t)}{N} = -\beta + \sqrt{(\beta - \beta_i)^2 + \frac{2}{N} \ln t}, \quad (53)$$

which is (accidentally) the same as (24). Then the final result is

$$\begin{aligned} \frac{\mathcal{E}(t)}{N} = & -\beta + \left( (\beta - \beta_i)^2 + \frac{2}{N} \ln \frac{t}{N} + \frac{2}{N} \ln C \left( \mathcal{E}^{(0)}(t) \right) \right. \\ & \left. + \frac{\beta - \beta_i}{N\beta_i} \ln (2\pi N\beta_i^2) - \frac{2\gamma\beta}{N\beta_i} + 2\frac{\beta}{N} (\phi(\inf I) - \inf I) \right)^{\frac{1}{2}}. \end{aligned} \quad (54)$$

We should note that the piecewise concatenation of these functions is not expected to give good results around  $t'_5$ . That is because the right hand side of (51) should actually be the same replacing  $t$  by  $t - t'_5$  and adding the right hand side of (47). However, the transition between the two expressions happens very quickly – just within a few times  $t'_5$ , which is nearly invisible on the rescaled plot. What is more, the expression should be further smoothed by the randomness of  $t'_5$ , which we took for constant.

### B.2.3 Original maximum

Now that we know  $\mathcal{E}(t)$ , we can use it to deduce  $\mathbb{E}[E_{\max}(t)|E(0)]$  and then obtain  $\mathbb{E}[E_{\max}(t)]$  by integrating over  $E(0)$ . Using (38) we get

$$\begin{aligned} \mathbb{E}[E_{\max}(t)] &= \mathbb{E}[\mathbb{E}[E_{\max}(t)|E(0)]] \approx \\ &\approx \int_{\inf I - T \ln t}^{\infty} \max(\mathcal{E}(t), E) \rho_{\text{gauss}}(E) dE + \int_{-\infty}^{\inf I - T \ln t} E \rho_{\text{gauss}}(E) dE = \\ &= \left( \operatorname{erfc} \left( \frac{\inf I - T \ln t}{\sqrt{N}} \right) - \operatorname{erfc} \left( \frac{\mathcal{E}(t)}{\sqrt{N}} \right) \right) \mathcal{E}(t) + \int_{|\mathcal{E}(t)|}^{T \ln t - \inf I} E \rho_{\text{gauss}}(E) dE \approx \\ &\approx \left( 1 - \operatorname{erfc} \left( \frac{\mathcal{E}(t)}{\sqrt{N}} \right) \right) \mathcal{E}(t) + \sqrt{\frac{N}{2\pi}} e^{-\frac{\mathcal{E}(t)^2}{2N}}, \end{aligned}$$

i.e.

$$\mathbb{E}[E_{\max}(t)] \approx \left( 1 - \operatorname{erfc} \left( \frac{\mathcal{E}(t)}{\sqrt{N}} \right) \right) \mathcal{E}(t) + \sqrt{\frac{N}{2\pi}} e^{-\frac{\mathcal{E}(t)^2}{2N}}, \quad (55)$$

which can be made explicit by plugging (43), (50) and (54) in it. This expression approaches  $\mathcal{E}(t)$  for large  $t$  and remains small as long as  $\mathcal{E}(t) < 0$ .

## B.3 Outlook on the finite- $N$ corrections

We analyzed preasymptotic corrections that should be taken into account in order to compare our predictions with numerical simulations. Because these corrections come from different sources, it was not possible to quantify their magnitude as some order of  $N$ . As we show at the end of this section, the corrections we accounted for are sufficient for a good match with numerical simulations. Still, it should be noted that there are several effects which we did not account for.

*Difference between  $E_{\min}(t)$  and  $E(t)$ .* An important source of error are the deviations from the theory of  $E_{\min}(t)$ , which were observed in [14]. Since our calculations are based on  $E_{\min}(t)$ , those are likely to have an impact here, too.

*Asymptotic statistics.* Eqs. (47) and (51) are only valid up to a factor of order 1 on the left hand side. Moreover, we arbitrarily used mean values for both  $\inf I$  and the Gumbel distribution, which should give errors on the effective value adapted to our observable of the order of their standard deviations.

*Time shift.* The correction introduced by using  $\phi$  [Eq. (40)] should also slightly impact the end of aging [Eq. (43)] and thereby the whole post-aging regime.

*Returns.* By considering the energies without memory of the trajectory’s history, we disregarded returns to recently visited traps, which dominate the dynamics at subexponential time scales [14]. Those should effectively increase the exit times from traps.

By comparing with numerical simulations (Fig. 4–left), one sees that the effects we neglected seem sufficiently unimportant. Theoretical and numerical curves follow the same trend without using any free parameter.

**Convergence to the asymptotic behavior** In figure Fig. 4–right we show the convergence of the finite-size  $E_{\max}(t)$  to its asymptotic limit, which is different depending on the regime. For long times,  $E_{\max}(t)$  becomes smaller with increasing  $N$ , and saturates at around  $N = 1000$ . At short times, the trend is inverted, and finite-size effects are sizeable for even larger system sizes. This slowness in the convergence explains why it is necessary to take into account finite-size corrections when comparing to numerical simulations.

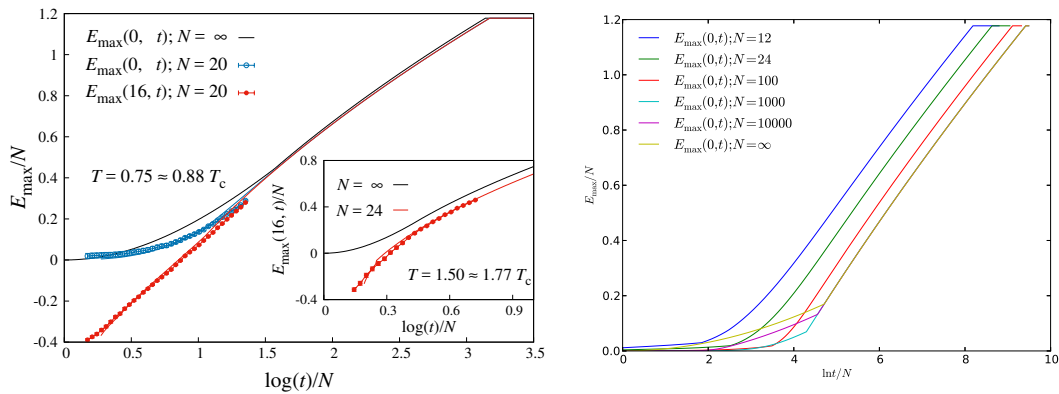


Figure 4: **Left:** Comparison between asymptotic solution, finite-size predictions and numerical simulations. We show analytical curve and numerical points for both  $E_{\max}(0, t)$  and  $E_{\max}(16, t)$ . We show  $T = 0.75 < T_c$  in the main figure, and  $T = 1.50 > T_c$  in the **inset**. **Right:** Convergence of the finite-size predictions for  $E_{\max}(0, t)$  to the asymptotic solution at  $T = 0.25 \approx 0.29T_c$ . Note that the convergence is non monotone and very slow, as we are deep in the glassy state. Moreover, the convergence after the equilibration time is faster.

## C Records in a single trajectory

Discussing the evolution of the maximum in a single trajectory can simplify the concepts that we exposed throughout the article. In Fig. 5 we show the evolution of the maximum reached energy, in a single trajectory. We use three different indicators:  $E_{\max}(0, t)$  is the maximum energy since the beginning of the run,  $E_{\max}(16, t)$  is a delayed maximum in which we wait 16 time steps before starting to record the maxima, in order to have the system fall in the first local minimum, and  $E_{\max}(t/2, t)$  is the maximum energy in the time window  $[t/2, t]$ . The latter has the advantage of showing very well the separation of time scales that occurs during the dynamics, since it takes into account increasingly larger time windows, and excludes configurations visited long before. In the run depicted, the initial state has  $E(0) \approx 0.2N$ , so  $E_{\max}(0, t)$  sticks to that value for a long time.  $E_{\max}(16, t)$ , instead, starts from a negative value, since in 16 time steps the system had the time to explore a portion of the landscape, lowering its energy. After around  $10^{10}$  MC steps  $E_{\max}(16, t)$  reaches  $E(0)$ , and, from that moment on,  $E_{\max}(16, t) = E_{\max}(0, t)$ . This is what would be the time  $t_3$ , marking the beginning of the First Records regime.

$E_{\max}(t/2, t)$  is the only indicator that can also decrease. It is equal to  $E_{\max}(16, t)$  either at the beginning of the run, when the system is stuck in the initial trap, or when new records are hit. As stated previously,  $E_{\max}(t/2, t)$  is a good separator of time scales. In fact, during the aging

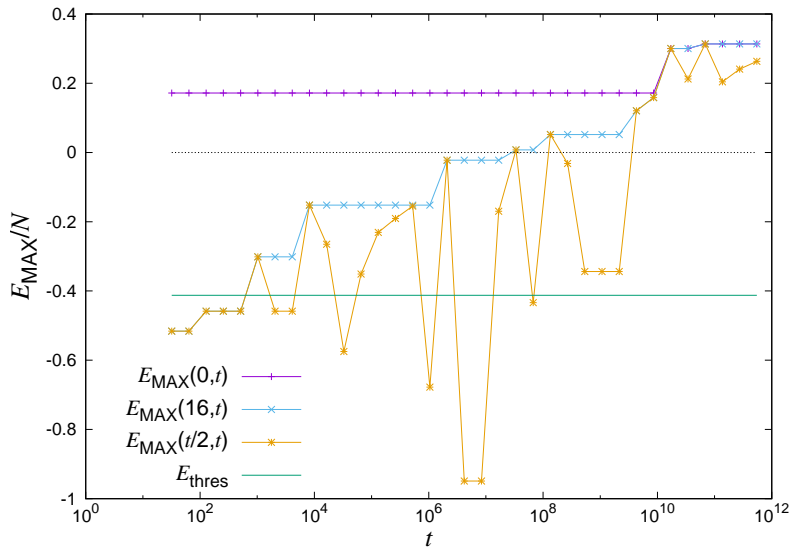


Figure 5: A random sample of the REM Metropolis dynamics, with  $N = 20$ ,  $T = 0.75$ . We show the maximal attained energy,  $E_{\max}(0, t)$ , the one disregarding the first 16 time steps,  $E_{\max}(16, t)$ , and the one between  $\frac{t}{2}$  and  $t$ ,  $E_{\max}(t/2, t)$ . The green horizontal line represents  $E_{\text{th}}$ . The black dashed horizontal line is a reference for  $E = 0$ .

stage,  $E_{\max}(t/2, t)$  goes several times under  $\inf I$ , indicating that the dynamics has accepted no move and has remained in the current trap for the considered interval.

## References

- [1] E. J. Gumbel. *Statistics of Extremes*. Columbia University Press, New York, 1958.
- [2] G. Schehr, S. N. Majumdar, G. Oshanin, and S. Redner. Exact record and order statistics of random walks via first-passage ideas. *First-Passage Phenomena and Their Applications*, 35:226, 2014.
- [3] S. Hallegatte, C. Green, R. J. Nicholls, and J. Corfee-Morlot. Future flood losses in major coastal cities. *Nature climate change*, 3(9):802–806, 2013.
- [4] G. Wergen. Records in stochastic processes—theory and applications. *J. Phys. A*, 46(22):223001, 2013.
- [5] I. M. Johnstone. Multivariate analysis and Jacobi ensembles: Largest eigenvalue, Tracy–Widom limits and rates of convergence. *Ann. Statist.*, 36(6):2638–2716, 12 2008.
- [6] S. Boettcher and P. Sibani. Comparing extremal and thermal explorations of energy landscapes. *Eur. Phys. J. B*, 44(3):317–326, 2005.
- [7] S. Boettcher and P. Sibani. Ageing in dense colloids as diffusion in the logarithm of time. *J Phys Condens Matter.*, 23(6):065103, 2011.
- [8] D. M. Robe, S. Boettcher, P. Sibani, and P. Yunker. Record dynamics: Direct experimental evidence from jammed colloids. *EPL (Europhysics Letters)*, 116(3):38003, 2016.
- [9] J. C. Dyre. Master-equation approach to the glass transition. *Phys. Rev. Lett.*, 58:792–795, Feb 1987.
- [10] J.-P. Bouchaud. Weak ergodicity breaking and aging in disordered systems. *J. Phys. I France*, 2:1705–1713, 1992.

- [11] C. Monthus and J.-P. Bouchaud. Models of traps and glass phenomenology. *J. Phys. A*, 29(14):3847, 1996.
- [12] B. Derrida. Random-energy model: Limit of a family of disordered models. *Phys. Rev. Lett.*, 45:79–82, Jul 1980.
- [13] B. Derrida. Random-energy model: An exactly solvable model of disordered systems. *Phys. Rev. B*, 24:2613–2626, Sep 1981.
- [14] M. Baity-Jesi, G. Biroli, and C. Cammarota. Activated aging dynamics and effective trap model description in the random energy model. *J. Stat. Mech. Theory Exp.*, (1):013301, 2018.
- [15] V. Gayrard. Aging in Metropolis dynamics of the REM: a proof. *Probab. Theory Related Fields*, Sep 2018.
- [16] A. Billoire, L. Giomi, and E. Marinari. The mean-field infinite range  $p = 3$  spin glass: Equilibrium landscape and correlation time scales. *EPL (Europhysics Letters)*, 71(5):824, 2005.
- [17] M. Baity-Jesi, A. Achard-de Lustrac, and G. Biroli. Activated dynamics: an intermediate model between REM and  $p$ -spin. *Phys. Rev. E*, 98:012133, 2018.
- [18] A. Crisanti and F. Ritort. Activated processes and inherent structure dynamics of finite-size mean-field models for glasses. *EPL (Europhysics Letters)*, 52(6):640, 2000.
- [19] G. Ben-Arous and J. Černý. Course 8 - dynamics of trap models. In A. Bovier, F. Dunlop, A. van Enter, F. den Hollander, and J. Dalibard, editors, *Mathematical Statistical Physics*, volume 83 of *Les Houches*, pages 331 – 394. Elsevier, 2006.
- [20] T. Castellani and A. Cavagna. Spin-glass theory for pedestrians. *J. Stat. Mech.*, 2005:P05012, 2005.
- [21] L. F. Cugliandolo and J. Kurchan. Analytical solution of the off-equilibrium dynamics of a long-range spin-glass model. *Phys. Rev. Lett.*, 71:173–176, Jul 1993.
- [22] T. Rizzo. Replica-symmetry-breaking transitions and off-equilibrium dynamics. *Phys. Rev. E*, 88:032135, Sep 2013.